This is "Advance Publication Article".
Received Date: 28 February 2020 Accepted Date: 18 August 2020
J-STAGE Advance published Date: 6 October 2020
Journal of Prosthodontic Research

Journal of Prosthodontic Research

Official Journal of Japan Prosthodontic Society

Original article

A simple solution to recycle and reuse dental CAD/CAM zirconia block from its waste residuals

Hao Ding[a], James Kit-Hon Tsoi[a*], Chi-wai Kan[b], Jukka P. Matinlinna[a]

[a] *Dental Materials Science, Discipline of Applied Oral Sciences and Community Dental Care, Faculty of Dentistry, The University of Hong Kong, Hong Kong SAR*
[b] *Institute of Textiles and Clothing, The Hong Kong Polytechnic University, Hong Kong SAR*

Abstract

Purpose: To seek a simple solution that can recycle and regenerate dental CAD/CAM zirconia green blanks from its waste residuals.
Methods: Waste residuals (3M® Lava™ Plus HT) were pulverized after dry milling and cutting, and subsequently sieved before pickling in a 0.5 M nitric acid. These powders were then dry-pressed and pre-sintered into blocks at seven different temperatures in the range 800−1100 °C. New zirconia blocks flagged with the same batch numbers were used as control. These blocks were cut into bars before subjected them to manufacturer-recommended sintering at 1450 °C. Crystalline phases (by XRD), elemental compositions (by EDX), surface morphologies (by SEM), machinability, linear shrinkage rate, relative density, and Knoop microhardness were evaluated before and after sintering, and four-point flexural strengths were also evaluated for the sintered zirconia bars.
Results: Only tetragonal phases were found in both pre- and fully-sintered recycled zirconia blocks. SEM results showed that pre-sintered samples at 950 °C had smooth and flat surfaces with evenly distributed particles. Recycled and control zirconia blocks had similar elemental compositions. Results from machined surface, linear shrinkage rate, relative density, and Knoop microhardness established that 950 °C and 1000 °C were suitable pre-sintering temperatures for recycling zirconia. Pre-sintered recycled zirconia had no significant differences in flexural strengths, however, samples pre-sintered at 1000 °C exhibited the closest value (897 MPa) compared to that of the control (904 MPa).
Conclusions: Dental CAD/CAM zirconia can be recycled and reused from its waste residuals by adopting a simple method that requires a pre-sintering at 950 or 1000 °C.

Keywords: *Zirconia, Dental materials, Recycle, Waste, CAD/CAM*

Received 28 February 2020, Accepted 18 August 2020, Available online 6 October 2020

1. Introduction

With many recent developments in modern science and technology, the overall quality of life, medical treatments, and life expectancy have been improved significantly. Consequently, the number and ratio of aging populations in the world are increasing [1]. The global percentages of people aged ≥ 60 years have increased from 9.2% in 1990 to 11.7% in 2013, and it is expected to reach 21.1% by 2050 [2]. In addition, with the improvements in living conditions and increasing competition in modern society, people are paying more attention to their appearances, and especially to their teeth. Hence, aesthetic dentistry is becoming increasingly popular, and there is a keen demand for better dental restoration materials. In the field of dental restorations, porcelain-fused-to-metal (PFM) restorations are commonly used whereas PFM exhibits satisfactory mechanical strength from the bottom metal layer. However, PFM manifests two prominent drawbacks: the metal part restricts the light transmittance of porcelain and can cause allergic reactions in the human body [3]. Subsequently, all-ceramic restorations have the advantages of aesthetics and biocompatibility, and thus, represent ideal materials for dental restoration.

High-performance ceramics provide good foundations for developing high strength all-ceramic dental materials, of which yttria-stabilized zirconia (YSZ) has been under intensive focus recently in the field of dentistry [4-13]. This material can be toughened by stress-induced transformations and has relatively higher strength and toughness than alumina ceramics. Besides, its mechanical properties, color, and stability make it an ideal material for dental restorations. Nevertheless, zirconia cannot be processed in a dental laboratory by traditional methods (e.g. powder or liquid application), and the processing of robust compact sintered zirconia is a time-consuming procedure that leads to high wear of the milling instruments [14]. Therefore, the fabrication of zirconia are commonly done on prefabricated blanks that require computer-aided design/computer-aided manufacturing (CAD/CAM) to design different dental structures,

* Corresponding author at: Faculty of Dentistry, The University of Hong Kong, Prince Philip Dental Hospital, 34 Hospital Road, Pokfulam, Hong Kong SAR
E-mail address: jkhtsoi@hku.hk (J.K.H. Tsoi).

https://doi.org/10.2186/jpr.JPR_D_20_00002

such as inlays, onlays, veneers, crowns, fixed partial dentures, and implant abutments [15,16], and machine into individual forms by milling processes. Subsequently, the structures are sintered at specific high temperatures to achieve the optimum mechanical strength. Since the sintering process of zirconia leads to shrinkage, specialized computer software [17] is necessary to compensate for the shrinkage effect by enlarging the original form prior to machining.

Similar to all CAD/CAM milling processes, dental zirconia milling dust (~30%) and block residuals (~80%) as wastes have been reported [18] that incur significant economic and environmental losses [19]. Therefore, an appropriate reuse of such zirconia wastes would certainly increase its eco-friendliness and cost efficiency. Gouveia et al. [19] attempted to recycle dental zirconia, but the recycled product can only be used in the jewelry industry. Therefore, in this study, we aim to seek an easy and clean method to recycle dental CAD/CAM zirconia green blank wastes that can be reused effectively for dental prostheses.

2. Materials and Methods

2.1. Recycling pre-treatment of zirconia discs

Wastes of 3M® Lava™ Plus High Translucency Zirconia discs (Lot: 579006, diameter: 98 mm, thickness: 25 mm) were collected from in-house laboratories. These residues were first powdered by a pulverizer (FS-100, Xin Li, China) using a speed of 10,000 rpm, and then sieved through a 325 mesh (48 μm) screen. The powders were soaked, mixed, and stirred properly in a 0.5 mol/L nitric acid for 5 min at 55 °C. Finally, the powders were cleaned thoroughly with distilled water and stored in a drying oven for future uses.

2.2. Dry Press of Green Zirconia Body

The dry pressing method, which is a simple process to form green blanks [20], was adopted in this study. Approximately 10.0 g of powder were weighed using an analytical balance (AT201, Mettler-Toledo, Switzerland) and poured into a custom-made rectangular stainless steel mold of dimensions 35.0 mm × 30.0 mm × 10.0 mm (Figure 1). The mold was compacted under a hydraulic press (Silfradent 660, Italy) using a force of 80 kN to achieve the final size of the recycled zirconia green body (35.0 mm × 30.0 mm × 3.0 mm). Finally, the recycled green body was dried in an oven for 24 h. A total of 21 green body blanks were produced and the dimensions of each pressed green body were recorded. Appropriate new zirconia discs with the same lot were also produced to use as control.

2.3. Sintering of Green Body

The recycled green body blocks were subjected to a pre-sintering process in a box furnace (XD-1700M, Brother, China). First, binders and other organic additives were removed by heating the samples to 600 °C using a slow heating ramp of 5 °C / min from room temperature. Then, for each pre-sintering temperature (800, 850, 900, 950, 100, 1050 and 1100 °C), three dry-pressed blanks were heated to the desired temperature from 600 °C at a rate of 10 °C / min. The heating duration was 2 h in each case before the sample was cooled naturally inside the furnace to room temperature. After that, the dimensions of each pre-sintered green body block were measured. Finally, the pre-sintered and control zirconia blocks were cut into 18 bars with dimensions of ~30.0 mm × 5.0 mm × 3.0 mm by using a cutting machine at dry conditions (ISOMET5000, Buehler, USA). Cross sectional pictures of cutting faces from all zirconia bar samples were taken in a 6500K lightbox.

The final stage of sintering was conducted following the manufacturer guidelines as follows. Both pre-sintered recycled green bodies and control zirconia bars were subjected to the same furnace heating: First, from room temperature to 800 °C at a rate of 20 °C/min, and then from 800 to 1450 °C at a rate of 10 °C/min with a holding time of 2 h. In the end, the samples were naturally cooled in the furnace. After that, the dimensions of each sintered sample were measured. Figure 2 shows the full heating curves of pre-sintering and sintering schemes implemented in this work.

2.4. Hardness, Linear Shrinkage, and Relative Density

The Knoop hardness of three randomly selected pre-sintered zirconia green bodies sintered at different temperatures as well as the respective fully sintered bar samples were tested by Leitz Micro-Hardness Tester (Leitz Inc. New York, USA) using 25 g and 50 g of loading forces with the help of a software (Leica QGo Software by Leica Microsystems Imaging Solutions Ltd., Wetzlar, Germany). The loading time of each sample was set as 10 s. Three different areas were tested on each bar specimen.

For the determination of linear shrinkages, length, width and thickness of a specimen at dry-pressed (n = 3), pre-sintered (n = 7), and fully sintered (n = 7) stages were measured by a slide caliper for three times and recorded. The linear shrinkage (L) was calculated by the following equation [21]:

$$\mathrm{L} = \frac{L_2 - L_1}{L_1} \times 100\% \quad (1)$$

Where:
L_1 = average length, width, or thickness of the sample before heating.
L_2 = average length, width, or thickness of the sample after presintering/sintering.

To estimate the relative density, three bar-shaped samples were randomly selected from the groups of zirconia green bodies pre-sintered at different temperatures as well as the respective fully sintered samples. In general, the following method was followed [22]: (1) weighing the sample dried in an oven, (2) using the boiling absorption method where the sample was put in a container completely submerged in distilled water, and boiled for 2 h, (3) the sample was then taken out of the boiling water and the surfaces were wiped off carefully to avoid absorption of water through the ceramic pores, and (4) weighing the sample immediately in air. The relative density (d) was calculated as follows:

$$d = \frac{m_1/(m_2 - m_1)}{d_0} \quad (2)$$

Where:
m_1 = sample's weight in air.
m_2 = sample's weight in air after fully submerged in water.
d_0 = theoretical density of the tetragonal phase of zirconia (d_0 = 6.10 g/cm^3).

2.5. Flexural Strength Test

Four-point bending tests were conducted in a universal testing machine (ElectroPuls™ E3000, Instron Industrial Products, Grove City, PA, USA) to determine the flexural strengths of seven randomly selected bar specimens from each group after the completion of the full sintering process. Before the test, all samples were polished by SiC abrasive papers (200-, 600-, and 2400- grit papers) to achieve the dimensions of ~24.0 mm × 4.0 mm × 2.0 mm, and the chamfer edges were made in accordance with ISO 6872 [23]. The compressive extension rate was set as 1.0 mm/min, the center-to-center distance between outer support rollers was 20.0 mm and the center-to-center distance between inner support rollers was 10.0 mm. The data was recorded by the console software (Instron Industrial Products, PA, USA).

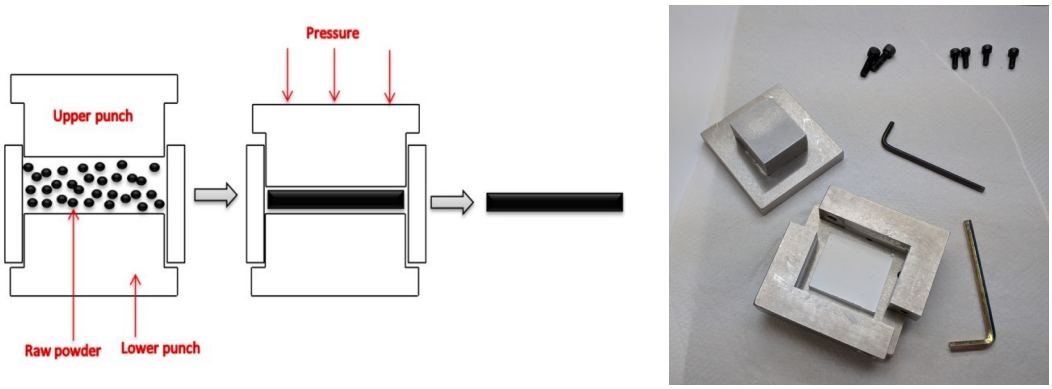

Fig. 1. Dry pressing process (left) and the detachable stainless steel mould used in this study (right).

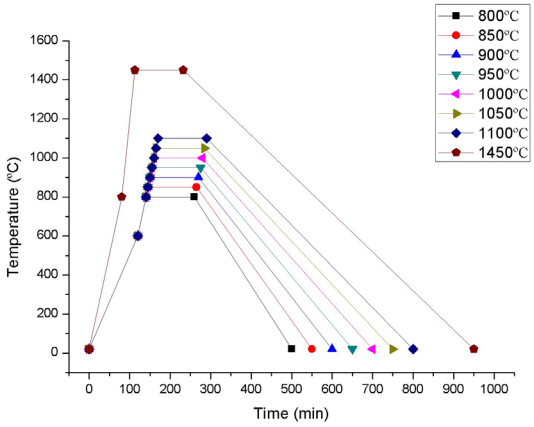

Fig. 2. Pre-sintering and final sintering programme curves of recycled zirconia block.

The flexural strength (σ) was calculated as follows:

$$\sigma = \frac{3PL}{4wb^2} \quad (3)$$

Where:
P = maximum load recorded in the software in Newton.
L = center-to-center distance between outer support rollers in millimeters.
w = width of the sample in millimeters (the dimension of the side at right angles to the direction of the applied load).
b = the thickness of the sample in millimeters (the dimension of the side parallel to the direction of the applied load).

2.6. X-ray Diffraction

X-ray diffractometer (SmartLab, Rigaku, Japan) was used to determine the crystalline phases (tetragonal and monoclinic) present in the recycled zirconia powder, recycled pre-sintered zirconia blocks and in the sintered zirconia blocks. Scans were performed at a rate of 1.00°/min in two thetas with a step-size of 0.02° using a source voltage of 40 kV and a current of 40 mA.

2.7. SEM and EDX

SEM (SU1510, Hitachi, Tokyo, Japan) and EDX (IXRF System Inc., Austin, TX, USA) were conducted on recycled zirconia powder and zirconia blocks for all different pre-sintering temperatures as well as on the respective fully sintered zirconia blocks. A thin gold layer was coated on each sample by an MSP-2S magnetron sputter. The coating duration was 3 min for all the samples.

2.8. Statistical Analysis

Mean values of the results were analyzed by one-way ANOVA using the software SPSS 23 (Chicago, IL, USA) with linear shrinkage, relative density, and Knoop hardness of pre-sintered and fully sintered samples including the flexural strength of fully sintered samples as dependent variables. Independent variables were different pre-sintering temperatures and the parameters of the control zirconia block. The level for all statistical significances was set as 0.05.

It should be noted that the percentile data were arcsine-transformed prior to ANOVA analyses. It is a typical data processing method for percentages ranges from 0 to 100% because the variances of means near 0 and 100% tend to be smaller than the variances of means in the middle of the range (30–70%) [24]. Hence, the percentages based on counts are discontinuous and have a binomial distribution. The arcsine-transformation is needed for error reductions in these types of data [25]. Arcsine-transformation converts the percentage to angle for which the equations are listed below:

$$Y' = \sin^{-1}\sqrt{Y} \quad (4)$$

Where:
Y = percentages in decimal fractions
Y' = transformed data in degree or radian

3. Results

3.1. X-ray Diffraction

Figure 3 shows the standard XRD peaks of monoclinic zirconia and tetragonal zirconia together with the measured diffraction patterns of recycled zirconia powder, pre-sintered and fully sintered zirconia blocks at 1000 °C. It can be concluded that the monoclinic phase exists only in pulverized zirconia, while no monoclinic phases can be detected for pre-sintered and fully sintered zirconia blocks.

3.2. Surface morphologies

3.2.1. SEM

Surface morphologies of the blocks from each group were examined using an SEM. For pre-sintered samples, ×250 magnification images

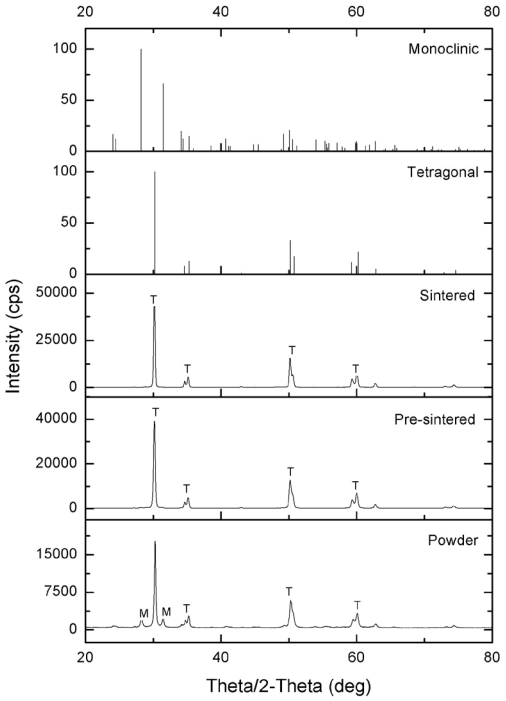

Fig. 3. XRD analysis results for recycled powder, pre-sintered at 1000°C, and its respective full-sintered state.

were captured to observe their surface roughness, while ×10000 magnification images were captured for the fully sintered samples to evaluate the particle size distributions. The serial SEM images (Figure 4) show the differences in surface topography among samples pre-sintered at different temperatures.

Figure 4(a) shows the control zirconia block. It can be observed that the surface of the original block was very flat and smooth. The image on the right depicts the control block after it was fully sintered at 1450 °C that evidently has a uniform distribution of particles. Figures 4 (b)-(h) show the surface morphologies of recycled zirconia blocks pre-sintered at respective temperatures of 800, 850, 900, 950, 1000, 1050 and 1100 °C. For the sample pre-sintered at 800 °C (Figure 4(b)), the surface appeared quite rough compared to the control sample surface and the quality of particle distribution was poor after it was fully sintered at 1450 °C. In addition to those non-uniform particle distributions, several small cracks or cleavages between particles could also be seen. These bad qualities of the surface structure can be directly related to the poor mechanical properties of the fully sintered products.

The samples pre-sintered at 850, 900, and 950 °C are shown respectively in Figures 4(c), 4(d), and 4(e). As the pre-sintering temperature increased, surfaces of the zirconia blocks became smoother, and more evenly distributed particles with a fewer number of cleavages between the particles were found in the corresponding fully sintered bodies for which the images are shown on the right.

However, for the samples pre-sintered at temperatures ≥ 1000 °C as presented in Figures 4(f)-(h), the surfaces look denser which may lead to more difficulties in the further machining process. In summary, it can be concluded from the SEM results that 950 °C seems to be a suitable temperature for pre-sintering of the samples.

3.2.2. Cutting surface morphologies

The cross-sectional pictures of the pre-sintered zirconia blocks are shown in Figure 5. It is evident that as the pre-sintering temperature increased, more scratches appeared on the cross-sectional surface areas, meaning that the machining became more challenging for them. By comparing the images with the control sample, it can be concluded that the wear degree of the control block was similar to the samples pre-sintered at 950 and 1000 °C.

3.2.3. Energy Dispersive X-ray Spectroscopy

EDX measurements were done on selected areas of zirconia powder and block samples after the imaging in the SEM. The magnification of the selected areas was set as 100 times. The results are shown in Figure 6.

The quantitative analysis of the EDX results established that the recycled blocks had a similar proportion of key elements such as zirconium, yttria, aluminum and oxygen compared to the control block and the powder. As each key element has a distinct role in the system, a different proportion of elements may induce different properties in a recycled block compared to the control block.

3.3. Linear Shrinkage

Figure 7 shows the linear shrinkage of pre-sintered zirconia blocks and fully sintered zirconia blocks. The black and red solid curves show the linear shrinkage rate of the pre-sintered and fully sintered zirconia blocks, respectively, while the red dashed line indicates the linear shrinkage rate of the control zirconia block.

The black solid curve shows the linear shrinkage rate of the pre-sintered zirconia block. Although the rate initially increased slowly from 800 to 950 °C, there was a sharp increase in the rate starting from the temperature 1000 °C. However, one-way ANOVA results (Table 1) revealed that there were significant differences ($p < 0.001$) among the samples pre-sintered at different temperatures in the range from 800 to 1100 °C in terms of their linear shrinkage rates.

For the fully sintered systems, recycled zirconia blocks showed a higher linear shrinkage rate compared to the control block. The red solid curve shows that once they were fully sintered, the linear shrinkage rate fluctuation was ~20%. The statistical analyses are shown in Table 2. It could be concluded that the result was significant at 0.05 level on post hoc multiple comparisons between fully sintered control blocks and recycled zirconia blocks with different pre-sintering temperatures. All recycled zirconia blocks showed a significantly higher value in linear shrinkage rate than the control sample ($p < 0.001$).

3.4. Relative Density

Figure 8 shows the relative densities of pre-sintered zirconia blocks and fully sintered zirconia blocks. The black and red solid curves show the relative densities of pre-sintered and fully sintered recycled zirconia blocks, respectively. The black dashed line shows the relative density of the control zirconia block before full sintering, while the red dashed line indicates the relative density of the fully sintered control zirconia block.

Similar to linear shrinkage rates, the relative densities of pre-sintered samples increased relatively slowly in the range from 800 to 950 °C. However, for temperatures ≥ 1000 °C, it exhibited a sharp increase. The one-way ANOVA results (Table 3) also indicate that there were significant differences in relative densities among samples pre-sintered at various temperatures ($p < 0.001$). This phenomenon can be related to the toughening mechanisms occurring primarily in the temperature range from 1000 to 1100 °C, which could lead to poorer machinable properties.

The red solid curve in Figure 8 shows that the relative density undulates around 95% for the fully sintered samples. From the statistical analysis results (Table 4), it could be concluded that with the level of significance set as 0.05, recycled zirconia samples pre-sintered at 900, 950, 1000, and 1050 °C had no significant difference in their relative densities after the full sintering process, indicating they had similar relative densities compared to what the control zirconia block showed.

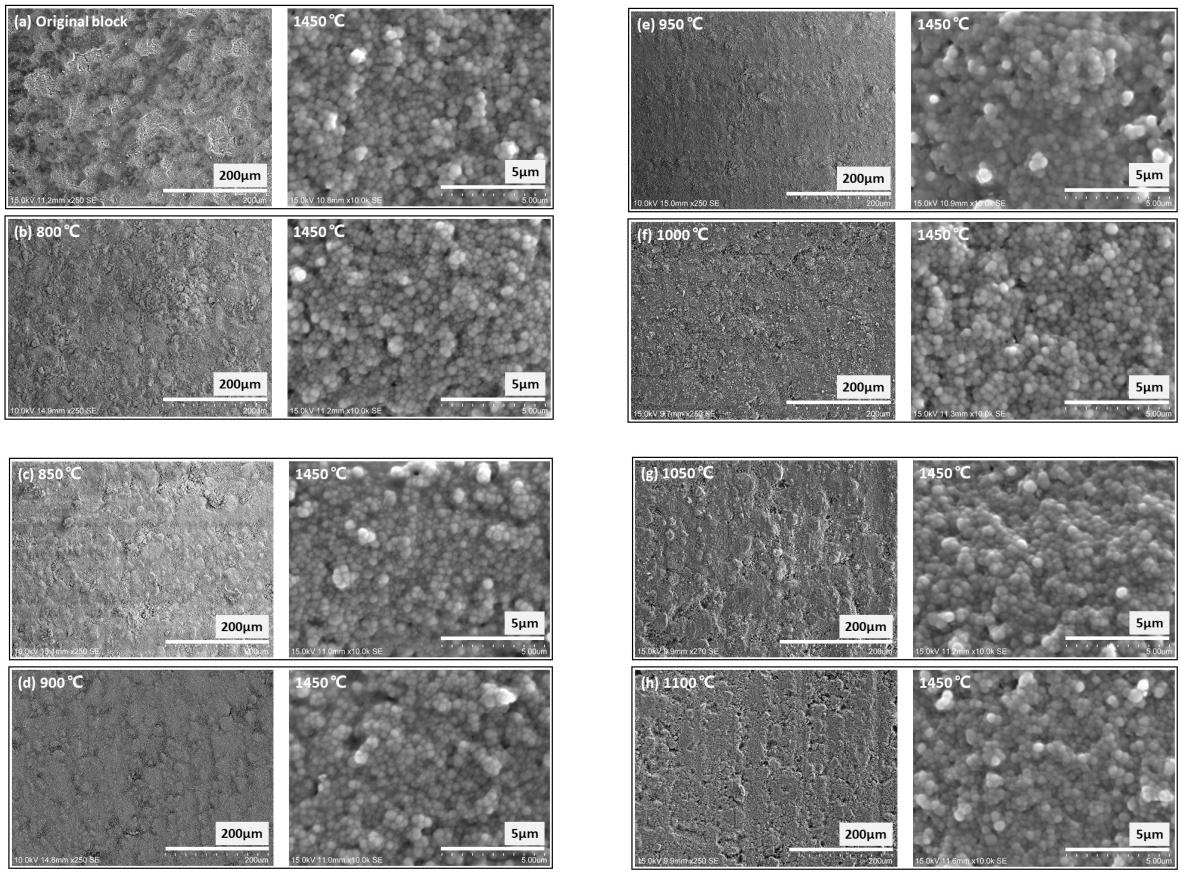

Fig. 4 . Representative surface topography of pre-sintered and fully sintered zirconia blocks, (a) original block, (b) pre-sintered at 800 °C, (c) pre-sintered at 850 °C, (d) pre-sintered at 900 °C, (e) pre-sintered at 950 °C, (f) pre-sintered at 1000 °C, (g) pre-sintered at 1050 °C and (h) pre-sintered at 1100 °C.

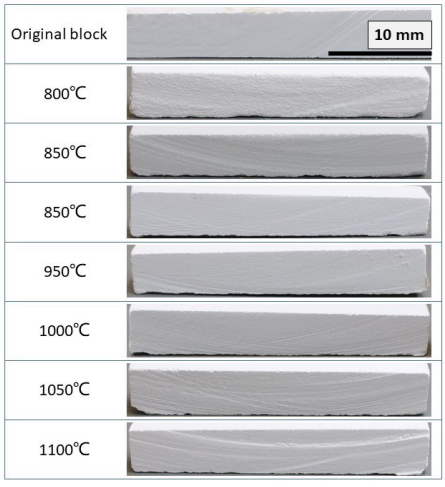

Fig. 5. Cross-section pictures of zirconia block with different pre-sintering temperatures.

3.5. Hardness

Figure 9 shows the results of Knoop hardness tests performed for different samples. The black solid curve and the black dashed line represent the hardness of the pre-sintered blocks and the control zirconia block, respectively. The red solid curve and the red dashed line show the hardness of fully sintered samples and fully sintered control block, respectively. In general, it shows nearly a linear correlation between pre-sintering temperatures and Knoop hardness values. The hardness of the control zirconia block before the full sintering was ~95 HK, which was very similar to the value obtained in the case of recycled zirconia block pre-sintered at 1000 °C.

One-way ANOVA analysis (Table 5) also proves the above observations. It shows that only the samples pre-sintered at 1000 °C had no significant differences at $p < 0.05$ compared to the control before full sintering. However, the results of one-way ANOVA (Table 6) shows that after full sintering the control block manifested a significantly higher Knoop hardness value than all the different samples pre-sintered at different temperatures. In addition, the red solid curve in Figure 8 shows that their final hardness after full sintering fluctuates around 980 HK. Although it is lower than the hardness of the control, it is large enough to be suitable for dental uses.

3.6. Flexural Strength

Figure 10 shows the four-point flexural strength of fully sintered recycled zirconia blocks (black solid line) and fully sintered control zirconia blocks (red solid line). Despite the results are quite large, the flexural strengths fall in the acceptable range especially for the samples pre-sintered at 950 and 1000 °C, for which the values are very close to the corresponding value of the control block (900 MPa). The results of one-way ANOVA (Table 7) also proved that there was no significant difference at the level of $p < 0.05$ between the flexural strengths of

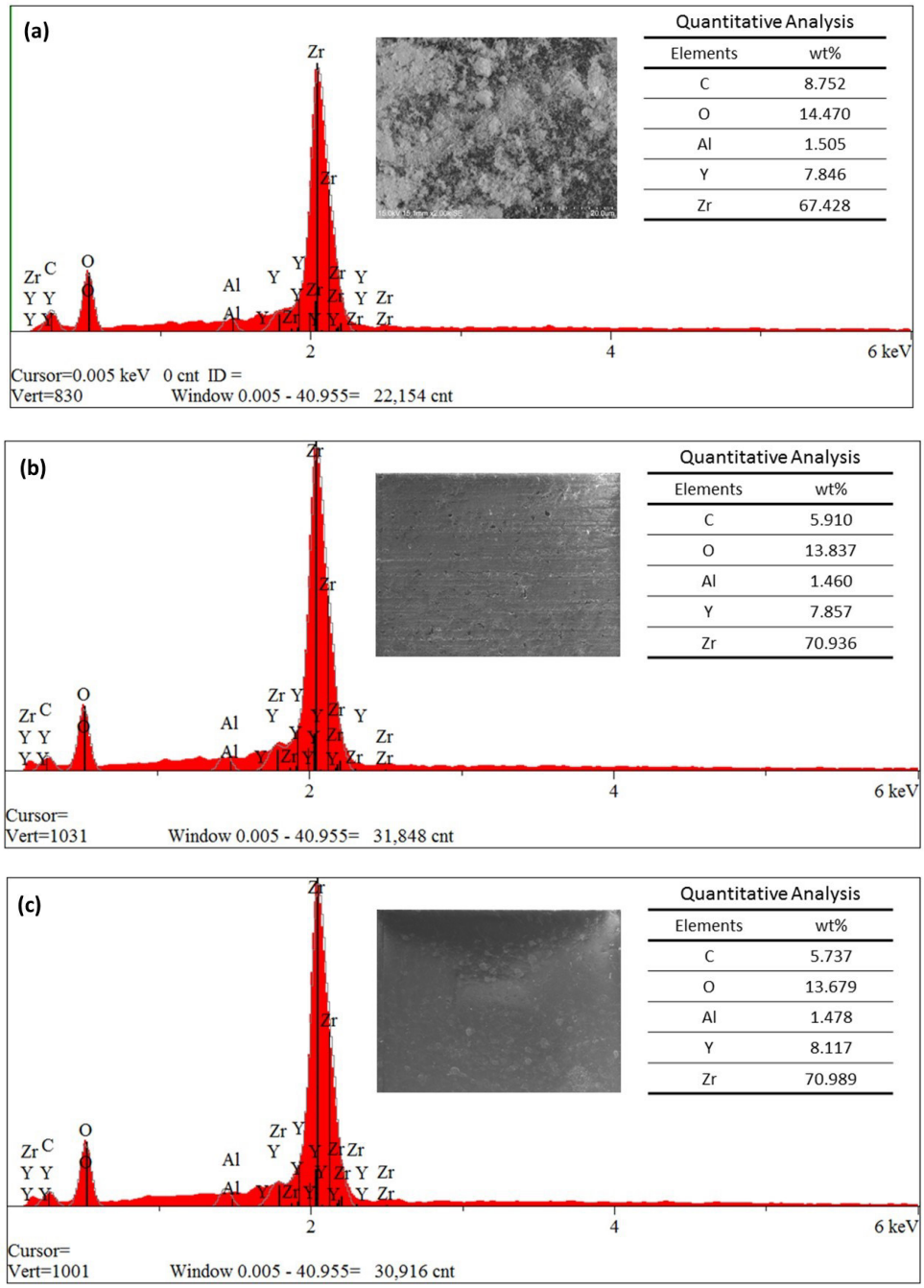

Fig. 6. Representative EDX analysis result for (a) zirconia powder, (b) recycled zirconia block pre-sintered at 950 °C, and (c) control zirconia block.

fully sintered control zirconia block and the recycled blocks pre-sintered at 950, 1000, and 1050 °C.

4. Discussion

In this study, as the experiment results indicate, dental zirconia waste residual blocks were successfully recycled with satisfactory properties. In particular, pre-sintering of the dry-pressed blocks at temperatures in the range 950−1000 °C deemed necessary to be suitable for dental applications requiring a certain level of flexural strength and the quality in surface topography.

The choice of the dry pressing method in this work was driven by the following two aspects: (1) its high production rate, and (2) its small dimensional tolerances leading to a better tolerance control. Dry pressing is one of the easiest techniques for powder compacting [20]. The most significant disadvantage of this method is the development of non-uniform density distributions as described in the literature.

However, this phenomenon mainly appears when a big mold is used for pressing. Hence, a smaller mold may not be much affected in this process.

It is well known that as different additives or impurities may exist in the green body, melting, decomposing, and volatilization of those additives or impurities could result in the deformation or craze in the ceramics which should be avoided. In fact, various impurities

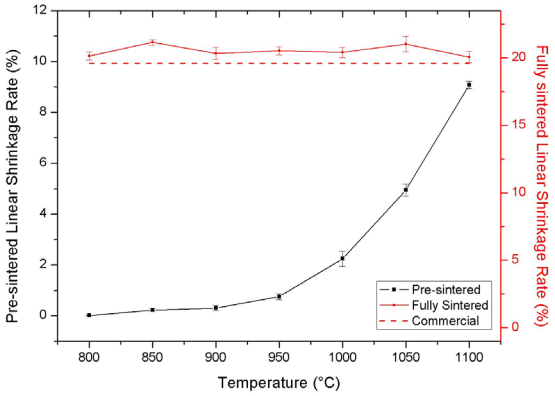

Fig. 7. Linear shrinkage rate of recycled zirconia block. The black and red solid curves shows the linear shrinkage rate of pre-sintered and fully sintered zirconia block, respectively. Red dashed line indicates the linear shrinkage rate of the control zirconia block.

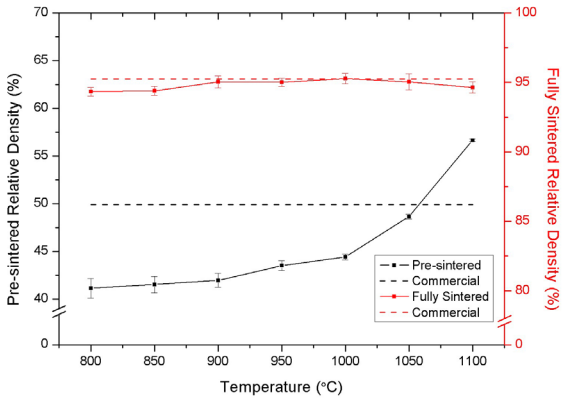

Fig. 8. Relative density of recycled zirconia block. The black and red solid curves shows the relative density of recycled pre-sintered and fully sintered zirconia block, respectively. The black and red dashed line shows the relative density of control zirconia block before and after fully sintered, respectively.

Table 1. One-way ANOVA analysis for pre-sintered linear shrinkage rate (percentile data were arcsine-transformed before ANOVA analysis).

	Sum of Squares	df	Mean Square	F	Sig.
Between Groups	1578.614	6	263.102	16848.992	.000
Within Groups	.656	42	.016		
Total	1579.269	48			

have been effectively removed by an acid pretreatment that was not detected from the EDX result. It is worth noting that the 5.7−8.7 wt.% of carbon content detected from the EDX were from the carbon tape used to attach the zirconia sample on the SEM/EDX mount. In addition, Han et al. [26] has shown in a recent study that carbon can always be found on zirconia surfaces due to the adsorption of atmospheric CO_2. Besides the temperature, heating rate and heating duration should have a major influence not only on the binder removal process but also in determining the final quality of the ceramics . Ding [27] have reported that during the sintering of zirconia, lower heating rates resulted in higher flexural strengths and hardness of the system. This may be attributed to the fact that a higher heating rate could shorten the crystallization period, and as a result, pores in between the grains cannot be excreted. Stages of mean weight loss appeared while the sintering temperature was below 600 °C, followed by a severe physicochemical reaction and a change of state. Binders or other additives were also removed during this period [28]. To prevent the occurrence of volatilizing gases expanding too fast and affecting the mechanical properties of the ceramics, a slower heating rate of 5 °C / min was set from the room temperature to 600 °C.

With regards to the linear shrinkage rate, relative density, and hardness test results, fully sintered recycled zirconia blocks exhibited very similar results compared to the control zirconia block. In addition, the above three physical parameters were greatly affected by the powder formation processes as well as by the sintering conditions. A higher and more evenly distributed pressure during the dry pressing method could make the ceramics have a smaller linear shrinkage rate, higher relative density, and greater hardness value, while a slower heating and cooling rate including a longer heating duration can further improve those properties. However, these adjustments in the processing mean an increased recycling cost with longer production times. Nonetheless, as the improvements in properties may not that obvious after achieving a certain level, further investigations are certainly needed to find an appropriate balance between the material's performance and the production cost.

It should be noted that no standard evaluation method exists for measuring the machinable properties. Boccaccini introduced a brittleness index (BI) to evaluate ceramic machinability [29], where :

$$\mathrm{BI} \sim \frac{Hardness\ (HV)}{Fracture\ toughness\ (K_{IC})}$$

Hardness is used to evaluate the ability to resist deformations of a material and fracture toughness is used to evaluate the ability to resist cracking in a material. The higher a material's brittleness index is, the poorer its machinability. Despite BI has been shown as a reliable evaluator with a marginal chipping factor in the cases of dental glass ceramics [30], determinations of HV and K_{IC} rely on indentation mechanics and BI is not suitable for zirconia [31] because zirconia is toughened by transformations that would resist crack formations and growth. Therefore, median cracks may not form during the indentation process, or the cracks would be much smaller than those naturally occurred in zirconia, or the cracks can also be very small that polishing would eliminate or severely reduced its size. Indeed, the ISO standard for dental ceramics (ISO 6872) has indicated that the determination of K_{IC} should not be relying on indentation hardness. Therefore, BI should not be utilized to determine the machinability of dental ceramics. Even though studies have shown machinability of a material can be determined by using removal rates during cutting, grinding force (P) measurement and cutting energy, where $P \propto [K_{IC}^{1/2}H^{5/8}/(E/H)^{4/5}]^{8/9}$ (E is elastic modulus) [32], those studies relied on indentation fracture mechanics and therefore it is useless in dental ceramics. In particular, chipping is one of the biggest problems in any dental zirconia restoration process [33]. Hence, a proper development to evaluate the machinability of dental CAD/CAM zirconia is indeed necessary.

The results of flexural strength tests should be stressed as it indicates that after the pre-sintering temperature reaches 1000 °C, the flexural strength was on a declining curve. Flexural strength is closely related to crack propagations, such that the initial crack of ceramic depends on the grain size because at initial stage the crack could only propagate into the nearer grains [34]. In addition, according the R-curve behavior in zirconia, the resistances of crack propagations would be greater for longer cracks [35]. For the hard-brittle materials like ceramics,

Table 2. One-way ANOVA analysis for fully sintered linear shrinkage rate (percentile data were arcsine-transformed before ANOVA analysis).

LSD post hoc test

					95% Confidence Interval	
(I)	(J)	Mean Difference (I-J)	Std. Error	Sig.	Lower Bound	Upper Bound
Control	800°C	-.40184164286*	.10253553157	.000	-.6080031465	-.1956801392
	850°C	-1.10874471571*	.10253553157	.000	-1.3149062194	-.9025832121
	900°C	-.53097136286*	.10253553157	.000	-.7371328665	-.3248098592
	950°C	-.67237009000*	.10253553157	.000	-.8785315937	-.4662085863
	1000°C	-.58502050857*	.10253553157	.000	-.7911820122	-.3788590049
	1050°C	-1.01797715143*	.10253553157	.000	-1.2241386551	-.8118156478
	1100°C	-.32926113143*	.10253553157	.002	-.5354226351	-.1230996278

*. The mean difference is significant at the 0.05 level.

Table 3. One-way ANOVA analysis for pre-sintered relative density (percentile data were arcsine-transformed before ANOVA analysis).

Dunnett T3 post hoc test

					95% Confidence Interval	
(I)	(J)	Mean Difference (I-J)	Std. Error	Sig.	Lower Bound	Upper Bound
Control	800 °C	5.05374934571*	.18673728264	.000	4.1876889935	5.9198096980
	850 °C	4.82701930143*	.12827476365	.000	4.2374276686	5.4166109343
	900 °C	4.57472126143*	.11520415210	.000	4.0473274023	5.1021151206
	950 °C	3.67894358143*	.08387305842	.000	3.3017677102	4.0561194526
	1000 °C	3.15935288571*	.04841427284	.000	2.9554426613	3.3632631101
	1050 °C	.72734278571*	.03803165800	.000	.5743142035	.8803713679
	1100 °C	-3.86649765857*	.02842421884	0.000	-3.9756589064	-3.7573364107

*. The mean difference is significant at the 0.05 level.

Table 4. One-way ANOVA analysis for fully sintered relative density (percentile data were arcsine-transformed before ANOVA analysis).

LSD post hoc test

					95% Confidence Interval	
(I)	(J)	Mean Difference (I-J)	Std. Error	Sig.	Lower Bound	Upper Bound
Control	800 °C	1.18715481143*	.17660420965	.000	.8320682492	1.5422413737
	850 °C	1.10330697429*	.17660420965	.000	.7482204120	1.4583935366
	900 °C	.28922269857	.17660420965	.108	-.0658638637	.6443092608
	950 °C	.32087817286	.17660420965	.075	-.0342083894	.6759647351
	1000 °C	-.05365034143	.17660420965	.763	-.4087369037	.3014362208
	1050 °C	.25897027143	.17660420965	.149	-.0961162908	.6140568337
	1100 °C	.79548939000*	.17660420965	.000	.4404028277	1.1505759523

*. The mean difference is significant at the 0.05 level.

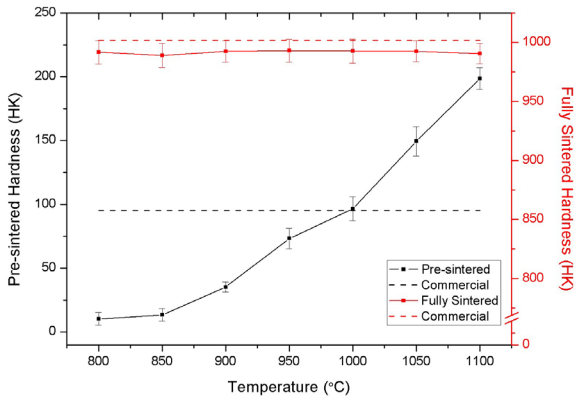

Fig. 9. Hardness of recycled zirconia block. The black solid curve and the black dashed line are the hardness of pre-sintered samples and control zirconia block, respectively, the red solid curve and the red dashed line are the hardness of fully sintered samples and control zirconia block after fully sintered, respectively.

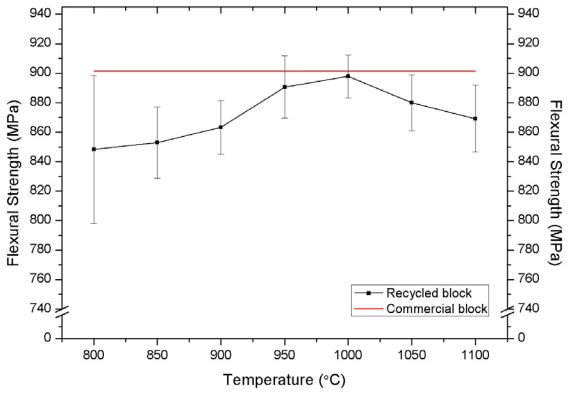

Fig. 10. Flexural strength of recycled zirconia block. The black solid curve shows the flexural strength of fully sintered recycled zirconia block, where the red solid line indicates the flexural strength of fully sintered control zirconia block.

Table 5. One-way ANOVA analysis for pre-sintered Knoop hardness.

LSD post hoc test

					95% Confidence Interval	
(I)	(J)	Mean Difference (I-J)	Std. Error`	Sig.	Lower Bound	Upper Bound
Control	800 °C	84.84857*	2.55321	.000	79.7150	89.9821
	850 °C	81.63000*	2.55321	.000	76.4964	86.7636
	900 °C	59.91000*	2.55321	.000	54.7764	65.0436
	950 °C	21.90000*	2.55321	.000	16.7664	27.0336
	1000 °C	-1.40143	2.55321	.586	-6.5350	3.7321
	1050 °C	-54.26143*	2.55321	.000	-59.3950	-49.1279
	1100 °C	-103.39143*	2.55321	.000	-108.5250	-98.2579

*. The mean difference is significant at the 0.05 level.

Table 6. One-way ANOVA analysis for fully sintered Knoop hardness.

LSD post hoc test

					95% Confidence Interval	
(I)	(J)	Mean Difference (I-J)	Std. Error	Sig.	Lower Bound	Upper Bound
Control	800 °C	10.17571*	3.67329	.008	2.7901	17.5614
	850 °C	12.87571*	3.67329	.001	5.4901	20.2614
	900 °C	9.56429*	3.67329	.012	2.1786	16.9499
	950 °C	8.91429*	3.67329	.019	1.5286	16.2999
	1000 °C	9.30571*	3.67329	.015	1.9201	16.6914
	1050 °C	9.40571*	3.67329	.014	2.0201	16.7914
	1100 °C	11.28571*	3.67329	.003	3.9001	18.6714

*. The mean difference is significant at the 0.05 level.

Table 7. One-way ANOVA analysis for fully sintered flexural strength.

LSD post hoc test

					95% Confidence Interval	
(I)	(J)	Mean Difference (I-J)	Std. Error	Sig.	Lower Bound	Upper Bound
Control	800 °C	53.1964571*	13.5279244	.000	25.996742	80.396172
	850 °C	48.4850429*	13.5279244	.001	21.285328	75.684758
	900 °C	38.2029000*	13.5279244	.007	11.003185	65.402615
	950 °C	10.8631714	13.5279244	.426	-16.336544	38.062887
	1000 °C	3.6326571	13.5279244	.789	-23.567058	30.832372
	1050 °C	21.5740143	13.5279244	.117	-5.625701	48.773729
	1100 °C	32.2430429*	13.5279244	.021	5.043328	59.442758

*. The mean difference is significant at the 0.05 level.

intergranular fracture is the main fracture mode. Small and irregular grain shapes make the propagation path longer, needing more energy for propagations which in fact help to improve the fractural strength of ceramics. However, as the ceramics were first pre-sintered at a relative high temperature, secondary crystallization may lead to unusual grain to growth. The larger grain size makes the total length of grain boundaries smaller, and as a result the effect of R-curve behavior gets reduced. In addition, from the linear shrinkage rate and the relative density results it was seen that the linear shrinkage rates and relative densities of zirconia samples pre-sintered below 1000 °C did not change much compared to the green bodies, which indicate that the grains did not start diffusing fully below 1000 °C, hence the abnormal grain growth appears only for the samples pre-sintered at temperatures > 1000 °C, which explains the drop in flexural strengths for the respective samples.

In summary, this paper describes a recycling method for dental zirconia ceramic wastes from the used blocks, especially suitable for the use in dental laboratories and for zirconia manufacturers. The advantages of this recycling method could be its short production cycle, high efficiency and cost effectiveness. In addition, it entails a simple manufacturing procedure and the recycled blocks exhibit very similar physical and chemical properties compared to the control sample. However, further improvements are required to produce larger and thicker recycled samples. Besides, the development of a universal sintering scheme suitable for different kinds of dental zirconia ceramics. Moreover, a standard quantitative measurement method should be developed for the cut surfaces. Further studies are also needed to examine aging behavior, bulk material's content of flaws, cracks and clinical trials of the restorations made from the recycled products.

5. Conclusion

We have developed a relatively simple, easy and clean method to recycle dental zirconia. It can be concluded that recycling dental zirconia CAD/CAM waste residuals from the used blocks is feasible with optimized pre-sintering temperatures in the range from 950 to 1000 °C.

Acknowledgements

This work was done in partial fulfillment of the requirements of the

degree of MSc(DMS) for the first author at the Faculty of Dentistry, The University of Hong Kong. The ceramic material was generously supplied by the manufacturer. Parts of the results have been reported in CED-IADR/NOF 2017 conference.

Conflict of Interest

Nil.

References

[1] Ettinger RL. The unique oral health needs of an aging population. Dental Clinics of North America 1997;41:633-49.
[2] United Nations. World Population Ageing 2013. ed.: United Nations Department of Economic and Social Affairs Population Division; 2013, p. of 95.
[3] Levi L, Barak S, Katz J. Allergic reactions associated with metal alloys in porcelain-fused-to-metal fixed prosthodontic devices-A systematic review. Quintessence Int 2012;43:871-7.
[4] Han A, Tsoi JKH, Matinlinna JP, Zhang Y, Chen Z. Effects of different sterilization methods on surface characteristics and biofilm formation on zirconia in vitro. Dent Mater 2018;34:272-81.
[5] Homaei E, Farhangdoost K, Tsoi JKH, Matinlinna JP, Pow EHN. Static and fatigue mechanical behavior of three dental CAD/CAM ceramics. J Mech Behav Biomed Mater 2016;59:304-13.
[6] Leung BT, Tsoi JK, Matinlinna JP, Pow EH. Comparison of mechanical properties of three machinable ceramics with an experimental fluorophlogopite glass ceramic. J Prosthet Dent 2015;114:440-6.
[7] Liu D, Tsoi JK, Matinlinna JP, Wong HM. Effects of some chemical surface modifications on resin zirconia adhesion. J Mech Behav Biomed Mater 2015;46:23-30.
[8] Liu D, Pow EHN, Tsoi JK, Matinlinna JP. Evaluation of four surface coating treatments for resin to zirconia bonding. J Mech Behav Biomed Mater 2014;32:300-9.
[9] Wong JD, Kei Lung CY, Tsoi JK, Matinlinna JP. Effects of a zirconate coupling agent incorporated into an experimental resin composite on its compressive strength and bonding to zirconia. J Mech Behav Biomed Mater 2014;29:171-6.
[10] Liu D, Matinlinna JP, Tsoi JK, Pow EH, Miyazaki T, Shibata Y, et al. A new modified laser pretreatment for porcelain zirconia bonding. Dent Mater 2013;29:559-65.
[11] Matinlinna JP, Choi AH, Tsoi JK. Bonding promotion of resin composite to silica-coated zirconia implant surface using a novel silane system. Clin Oral Implants Res 2013;24:290-6.
[12] Ho CMB, Ding H, Chen X, Tsoi JKH, Botelho MG. The effects of dry and wet grinding on the strength of dental zirconia. Ceramics International 2018;44:10451-62.
[13] Han A, Tsoi JKH, Lung CYK, Matinlinna JP. An introduction of biological performance of zirconia with different surface characteristics: A review. Dent Mater J 2020.
[14] Sailer I, Feher A, Filser F, Luthy H, Gauckler LJ, Scharer P, et al. Prospective clinical study of zirconia posterior fixed partial dentures: 3-year follow-up. Quintessence International-English Edition- 2006;37:685.
[15] Davidowitz G, Kotick PG. The Use of CAD/CAM in Dentistry. Dental Clinics of North America 2011;55:559-70.
[16] Miyazaki T, Nakamura T, Matsumura H, Ban S, Kobayashi T. Current status of zirconia restoration. J Prosthodont Res 2013;57:236-61.
[17] Filser F, Kocher P, Weibel F, Lüthy H, Schärer P, Gauckler L. Reliability and strength of all-ceramic dental restorations fabricated by direct ceramic machining (DCM). International Journal of Computerized Dentistry 2001;4:89-106.
[18] Tao J, Chen ZR, Yu SR, Liu ZF. Integration of Life Cycle Assessment with computer-aided product development by a feature-based approach. Journal of Cleaner Production 2017;143:1144-64.
[19] Gouveia PF, Schabbach LM, Souza JCM, Henriques B, Labrincha JA, Silva FS, et al. New perspectives for recycling dental zirconia waste resulting from CAD/CAM manufacturing process. Journal of Cleaner Production 2017;152:454-63.
[20] Li J, Pan Y, Zeng Y, Liu W, Jiang B, Guo J. The history, development, and future prospects for laser ceramics: A review. International Journal of Refractory Metals and Hard Materials 2013;39:44-52.
[21] Kleinlogel C, Gauckler L. Sintering and properties of nanosized ceria solid solutions. Solid State Ionics 2000;135:567-73.
[22] Yan G, Qiang ZF, Hui H, Yuan L, Ying L. Sintering behavior of Y-doped ZrO_2 ceramics: the effect of additive rare earth oxides. J Ceram Process Res 2008;14:270-6.
[23] ISO 6872. Dentistry - Ceramic Materials. ed., Geneva, Switzerland: International Organization for Standardization; 2008.
[24] Finney D. Was this in your statistics textbook? V. Transformation of data. Experimental Agriculture 1989;25:165-75.
[25] Fernandez GC. Residual analysis and data transformations: important tools in statistical analysis. HortScience 1992;27:297-300.
[26] Han AF, Ding H, Tsoi JKH, Imazato S, Matinlinna JP, Chen ZF. Prolonged UV-C Irradiation is a Double-Edged Sword on the Zirconia Surface. ACS Omega 2020;5:5126-33.
[27] Ding Y. An experiment of the effect of different heating rate on properties of zirconia ceramic for CAD/CAM. ed.: Fudan University; 2012, p. of 29.
[28] Hu L, Wang C-A. Effect of sintering temperature on compressive strength of porous yttria-stabilized zirconia ceramics. Ceramics international 2010;36:1697-701.
[29] Boccaccini A. Machinability and brittleness of glass-ceramics. Journal of Materials Processing Technology 1997;65:302-4.
[30] Tsitrou EA, Northeast SE, van Noort R. Brittleness index of machinable dental materials and its relation to the marginal chipping factor. Journal of dentistry 2007;35:897-902.
[31] Swab JJ, Tice J, Wereszczak AA, Kraft RH. Fracture Toughness of Advanced Structural Ceramics: Applying ASTM C1421. Journal of The American Ceramic Society 2015;98:607-15.
[32] Malkin S, Hwang T. Grinding mechanisms for ceramics. CIRP Annals-Manufacturing Technology 1996;45:569-80.
[33] Zhang Y, Chai H, Lee JJW, Lawn BR. Chipping Resistance of Graded Zirconia Ceramics for Dental Crowns. J Dent Res 2012;91:311-5.
[34] Miller K. Materials science perspective of metal fatigue resistance. Materials science and technology 1993;9:453-62.
[35] Heimann RB. Classic and advanced ceramics: from fundamentals to applications. John Wiley & Sons; 2010.